MicroRNAs Establish Robustness and Adaptability of a Critical Gene Network to Regulate Progenitor Fate Decisions during Cortical Neurogenesis

Tanay Ghosh, Julieta Aprea, Jeannette Nardelli, Hannes Engel, Christian Selinger, Cedric Mombereau, Thomas Lemonnier, Imane Moutkine, Leslie Schwendimann, Martina Dori, et al.

Cell Reports
Report

MicroRNAs Establish Robustness and Adaptability of a Critical Gene Network to Regulate Progenitor Fate Decisions during Cortical Neurogenesis

Tanay Ghosh,[1,2,3] Julieta Aprea,[4] Jeannette Nardelli,[5,6] Hannes Engel,[7] Christian Selinger,[8] Cedric Mombereau,[1,2,3] Thomas Lemonnier,[1,2,3] Imane Moutkine,[1,2,3] Leslie Schwendimann,[5,6] Martina Dori,[4] Theano Irinopoulou,[1,2,3] Alexandra Henrion-Caude,[9] Arndt G. Benecke,[10,11] Sebastian J. Arnold,[7,13] Pierre Gressens,[5,6,12] Federico Calegari,[4] and Matthias Groszer[1,2,3,*]

[1]Inserm, UMR-S839, Paris 75005, France
[2]Sorbonne Universités, UPMC Université Paris 06, Paris 75005, France
[3]Institut du Fer à Moulin, Paris 75005, France
[4]Center for Regenerative Therapies, TU-Dresden, Fetscherstraße 105, 01307 Dresden, Germany
[5]Inserm, U1141, Paris, 75019, France
[6]Université Paris Diderot, Sorbonne Paris Cité, UMRS 1141, Paris 75019, France
[7]Renal Department, University Medical Center, Breisacher Strasse 66, Freiburg 79106, Germany
[8]Department of Microbiology, School of Medicine, University of Washington, Seattle, WA 98195-8070, USA
[9]Inserm, UMR1163, GenAtlas, Institute Imagine, Université Paris Descartes, Paris 75015, France
[10]Institut des Hautes Etudes Scientifiques, Bures sur Yvette 91440, France
[11]CNRS UMR 7224, Université Pierre and Marie Curie, Paris 75005, France
[12]Centre for the Developing Brain, King's College, St Thomas' Campus, WC2R2LS London, UK
[13]BIOSS Centre of Biological Signalling Studies, Albert-Ludwigs-University, Freiburg 79085, Germany
*Correspondence: matthias.groszer@inserm.fr
http://dx.doi.org/10.1016/j.celrep.2014.05.029

SUMMARY

Over the course of cortical neurogenesis, the transition of progenitors from proliferation to differentiation requires a precise regulation of involved gene networks under varying environmental conditions. In order to identify such regulatory mechanisms, we analyzed microRNA (miRNA) target networks in progenitors during early and late stages of neurogenesis. We found that cyclin D1 is a network hub whose expression is miRNA-dosage sensitive. Experimental validation revealed a feedback regulation between cyclin D1 and its regulating miRNAs miR-20a, miR-20b, and miR-23a. Cyclin D1 induces expression of miR-20a and miR-20b, whereas it represses miR-23a. Inhibition of any of these miRNAs increases the developmental stage-specific mean and dynamic expression range (variance) of cyclin D1 protein in progenitors, leading to reduced neuronal differentiation. Thus, miRNAs establish robustness and stage-specific adaptability to a critical dosage-sensitive gene network during cortical neurogenesis. Understanding such network regulatory mechanisms for key developmental events can provide insights into individual susceptibilities for genetically complex neuropsychiatric disorders.

INTRODUCTION

During cortical development, the fate choice of progenitors to proliferate or to differentiate is precisely regulated to generate developmental stage-specific neuronal numbers and specifications. Though this process is guided by intrinsic and extrinsic signals, the gene networks that are critically involved in this cell-fate decision must be stable and widely insensitive to fluctuation of these signals (Enver et al., 2009). However, regulatory mechanisms that confer robustness and developmental-stage-specific adaptability to such gene networks are largely unknown.

MicroRNAs (miRNAs) regulate gene expression through post-transcriptional silencing of target mRNAs. While miRNAs are evolutionary highly conserved, their effect on specific target inhibition, however, tends to be quantitatively modest (Selbach et al., 2008; Baek et al., 2008). This led to suggestions that miRNAs serve in tuning and buffering gene expression in regulatory networks to canalize developmental processes (Staton et al., 2011; Li et al., 2009; Wu et al., 2009; Hornstein and Shomron, 2006). In tuning, miRNAs might set mean expression levels, whereas in buffering, they reduce the dynamic expression range of their targets (Wu et al., 2009).

Homozygous knockout of the miRNA processing enzyme Dicer or a few specific miRNAs has provided evidence for the crucial functions of miRNAs during cortical neurogenesis (Nowakowski et al., 2013; Bian et al., 2013). However, for most individual miRNAs, their roles in specific gene regulatory networks remain elusive (Volvert et al., 2012). Moreover, in such networks, multiple miRNAs may regulate via feedback or feedforward

relations the expression of the same critical mRNA by directly targeting its 3′ UTR (Tsang et al., 2007; Wu et al., 2010). Revealing such regulatory functions of miRNA provides fundamental insights into the emerging properties of neurodevelopmental gene networks.

Here, we analyzed genome-wide miRNA and mRNA expression of neural progenitors at early and late stages of cortical development to derive a gene regulatory network. We found that the dynamic expression of the critical network hub over the period of neurogenesis is regulated through the integration of different miRNA feedback loops. Our data demonstrate that both tuning and buffering functions of miRNAs impart stability and adaptability to this network to regulate the transition from progenitor to neuron.

RESULTS AND DISCUSSION

Over the period of cortical development, the majority of neurons for lower and upper cortical layers arise sequentially from basal progenitors (also named intermediate progenitors). These progenitors specifically express the transcription factor Tbr2 (Englund et al., 2005). We isolated basal progenitors from $Tbr2^{GFP}$ reporter mice (Arnold et al., 2009) by fluorescence-activated cell sorting (FACS) at embryonic day 13 (E13) and E16, corresponding to peak times of lower and upper layer neurogenesis, respectively (Caviness, 1982) (Figures S1A and S1B). Microarray analyses revealed the differential expression of 19 miRNAs and 1,501 mRNAs between E13 and E16 (Figures S1C and S1D). To identify developmental-stage specifically adapted miRNA target networks, we extracted metapredicted targets of these 19 miRNAs among the differentially expressed mRNAs and found a significant ($p = 1.23 \times 10^{-8}$, hypergeometric test) overlap of 25% (371 out of 1,501). These 371 mRNAs (Table S1) were collectively named differentially expressed putative miRNA targets (DPMTs). These DPMTs, but not the complementary set of differentially expressed mRNAs (CSDMs), showed significant overrepresentation for microcephaly/macrocephaly endophenotypes in humans (Figure S1E), suggesting important roles in brain-size development. To identify functional relations among DPMT genes, we used weighted gene coexpression network analysis (WGCNA) (Oldham et al., 2008). We identified three modules of highly coregulated genes (Figure 1A), which were significantly correlated with both stages of development (Figure 1A; Figure S1F). Gene ontology (GO) analysis revealed that the blue module was overrepresented for the KEGG (Kyoto Encyclopedia of Genes and Genome) pathway term "cell cycle" (Figure 1A) and contained *Ccnd1* (encoding for cyclin D1 protein). In addition, molecular network analysis (Pathway studio) of DPMTs yielded *Ccnd1* as hub gene with the highest indegree (Figure 1B).

DPMT networks (Figures 1A and 1B) might be sensitive to altered miRNA dosage. Notably, haploinsufficiency of the miR-17–92 cluster (containing miR-20a) was recently detected in a patient with Feingold syndrome and microcephaly (de Pontual et al., 2011). In mice, cortex-specific homozygous deletion of the miR-17–92 cluster disrupts neuron production at late developmental stages. This results in reduced cortical thickness, which was most pronounced at postnatal day 10 (P10) (Bian et al., 2013). To assess a dosage-sensitive effect of each differentially expressed miRNA individually is technically limiting. Therefore, we studied mice carrying a conditional heterozygous mutation of the miRNA processing enzyme Dicer (*Nestin-Cre*$^{+}$, *Dicer* $^{loxP/+}$, or *Dicer*$^{+/-}$). We analyzed first the behavior of *Dicer*$^{+/-}$ mice to robustly detect haploinsufficiency. Open-field and elevated plus maze tests of adult *Dicer*$^{+/-}$ mice revealed hypolocomotion and increased anxiety, respectively, suggesting that altered miRNA dosage causes behavioral abnormalities (Figures 2A and 2B). To assess neuron production, we injected bromodeoxyuridine (BrdU) at E16 and analyzed the number of BrdU+ neurons at P10. We observed a significant reduction (Figure 2C) of BrdU+ neurons in upper cortical layers of *Dicer*$^{+/-}$ heterozygous mice, suggesting that neurogenesis is miRNA-dosage sensitive. We next assessed cyclin D1 protein levels in the *Dicer*$^{+/-}$ cortex. We found that expression level and variance of cyclin D1 in E16 *Dicer*$^{+/-}$ cortical progenitors is increased (Figure 2D), indicating that the network hub (Figure 1B) is miRNA-dosage sensitive.

We and others previously demonstrated that cyclin D1 is a key driver of progression through the G1 cell-cycle phase in cortical progenitors (Pilaz et al., 2009; Lange et al., 2009). G1 length progressively increases with developmental stage (Salomoni and Calegari, 2010; Dehay and Kennedy, 2007), while cyclin D1 levels decrease. Overexpression of cyclin D1 in cortical progenitors in vivo prevents lengthening of G1 and inhibits the transition from proliferation to neuronal differentiation. Thus, cyclin D1 expression levels in progenitors require precise control at different developmental stages.

Therefore, we focused on miRNAs that potentially regulate cyclin D1. Among the differentially expressed miRNAs, miR-20a, miR-20b, and miR-23a have putative target sites in the 3′ UTR of *Ccnd1* and show reduced expression in *Dicer*$^{+/-}$ E16 cortex (Figure S2A). miR-20a and miR-20b (miR-20a/b) are predicted to target an identical sequence in the 3′ UTR. miR-20a/b, miR-17, and miR-106 are members of the same miRNA family based on seed sequence similarity and might show functional redundancy. However, miR-17 and miR-106 were not differentially expressed between E13 and E16 (Figure S2B). Furthermore, the expression levels of miR-17 and miR-106 were 45 and two times lower, respectively, when compared to miR-20a (Figure S2B). The differential expression patterns of these family members may suggest their functional specialization (Sieber et al., 2007). Expression of miRNA-20a/b and miR-23a in cortical progenitors were further verified by in situ hybridization (Figure S2C). Microarray and quantitative PCR (qPCR) analysis confirmed that Ccnd1 expression was higher at E13 than at E16 (Figure S1D) and corresponded with cyclin D1 protein levels (Figure S1G). miR-20a/b showed a positive correlation with cyclin D1 expression, while miR-23a was negatively correlated (Figure 3A; Figure S1D). Based on the expression correlations between these miRNAs and their putative target, cyclin D1 may be linked to miR-20a/b via a negative feedback loop and to miR-23a via a double negative feedback loop (Figure 3A). Characteristically, negative feedback loops reduce variance, whereas double negative feedback loops set the mean level of target expression (Wu et al., 2009). Here, these two loops are integrated via cyclin D1. Mathematical modeling of this integrated

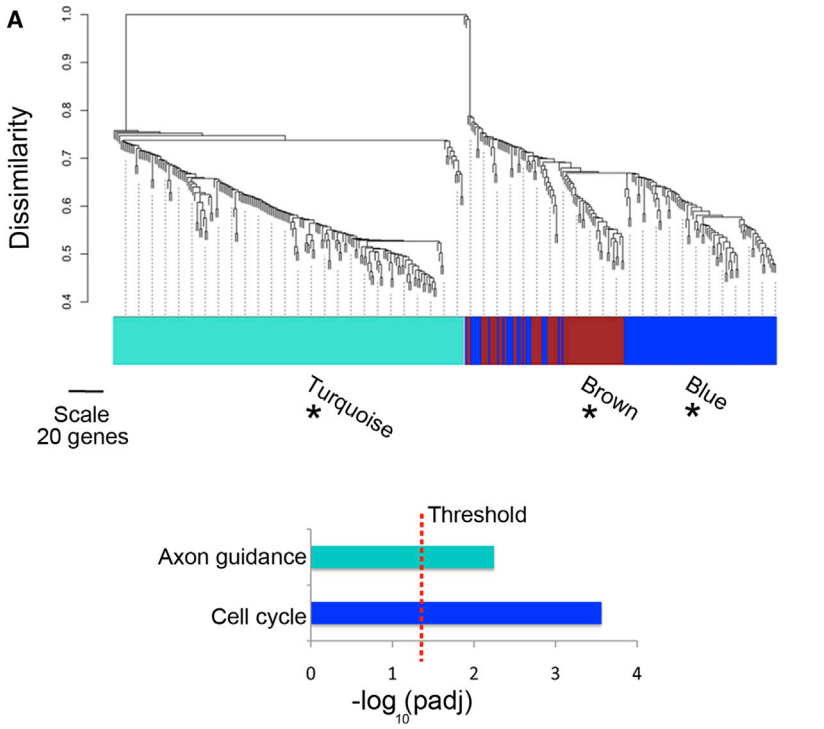

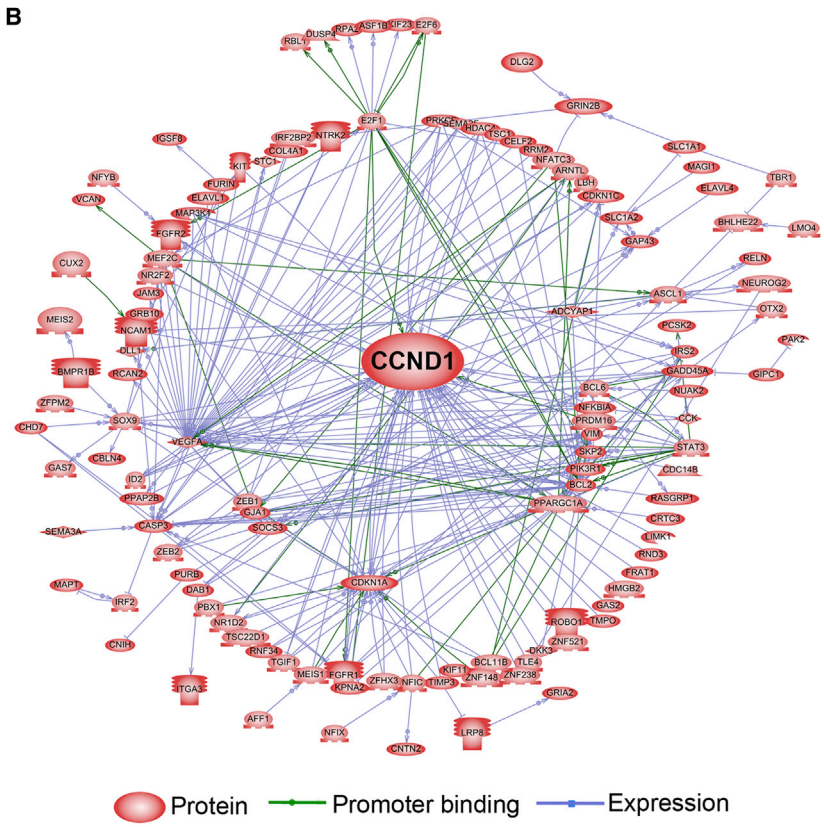

Figure 1. Network Analyses of DPMT

(A) Top: clustering dendrogram of DPMT and derived modules (colors labeled) after WGCNA. *p < 0.008 (Bonferroni threshold) for correlation of modules with developmental stages (see also Figure S1F and Table S1). Bottom: KEGG pathway terms, which are significantly overrepresented in modules. Threshold: Bonferroni adjusted p value 0.05.

(B) DPMT forms a molecular network with cyclin D1 as a hub with the highest indegree. Network genes are related through expression level and promoter binding data curated in Resnet database (Ariadne genomics).

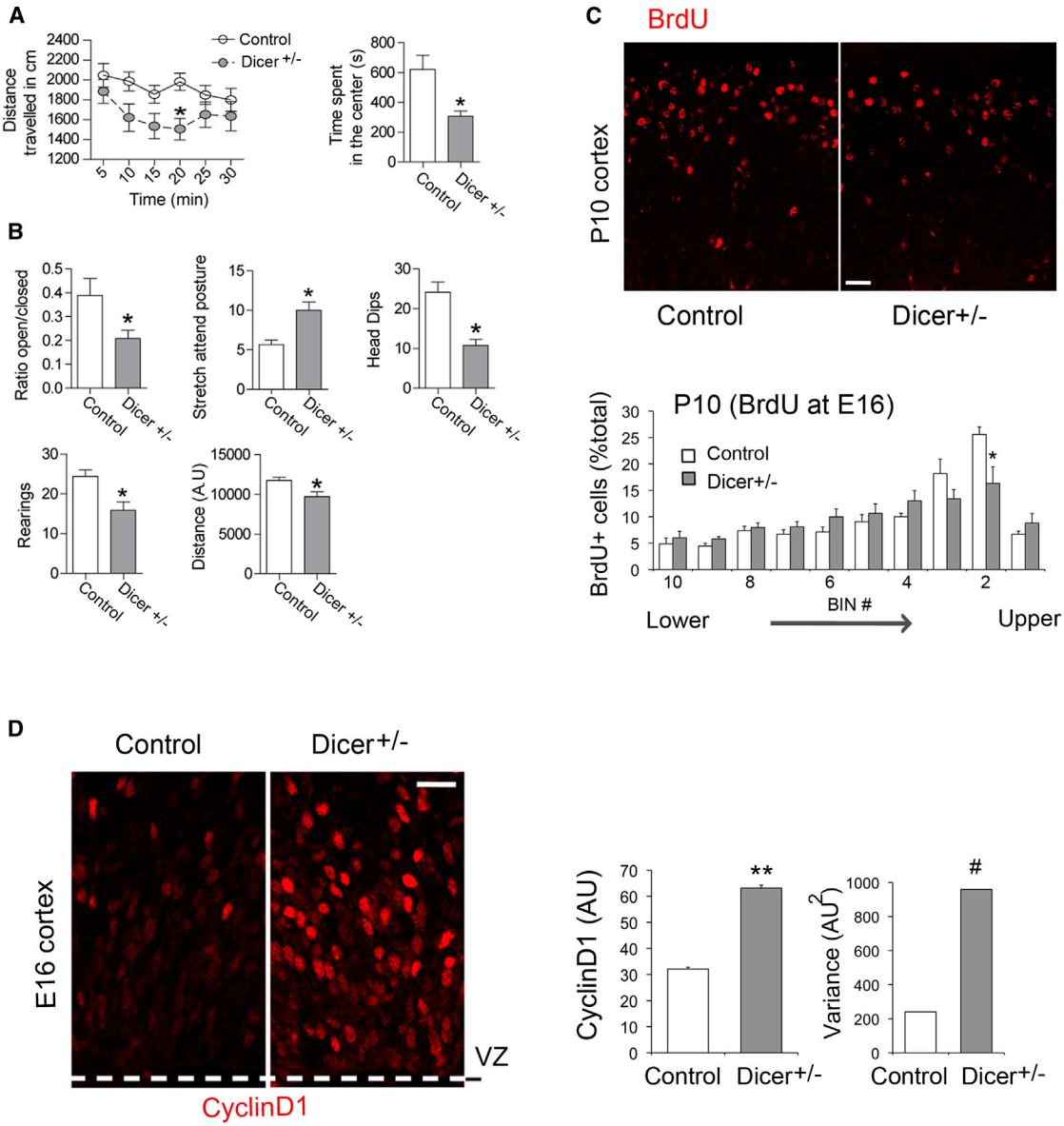

Figure 2. MiRNA Dosage Sensitivity in Conditional *Dicer*$^{+/-}$ Mice

(A and B) Behavioral tests in *Dicer*$^{+/-}$ mice (*Nestin-Cre*$^{+}$, *Dicer*$^{loxP/+}$) and control littermates (*Nestin-Cre*$^{-}$, *Dicer*$^{loxP/+}$). (A) Open-field tests revealed hypolocomotion (left) in heterozygotes. *p < 0.05, two-way ANOVA repeated measures (Bonferroni post test). In addition, *Dicer*$^{+/-}$ mice spent less time in the center (right), suggesting increased anxiety. *p < 0.05, Student's t test; n = 10–16 animals. (B) The elevated plus maze confirmed an increased anxiety in *Dicer*$^{+/-}$ mice, indicated by a decreased ratio of the time spend between open and closed arms and the smaller distance traveled in the maze. This was consistent with quantification of ethological markers of anxiety such as increased number of stretch attend postures and decreased number of head dips and rearings. *p < 0.05, Student's t test. n = 9–14 animals.

(C) Impaired cortical neurogenesis in Dicer$^{+/-}$ mice. BrdU-labeled neurons at E16 were counted at P10. *p < 0.05, ANOVA (Bonferroni post test), n = 4–6 animals. Representative BrdU labeling is shown.

(D) Immunofluorescence image (left) and quantification (right) of cyclin D1 mean level and variance in cortical progenitors in *Dicer*$^{+/-}$ mice. **p < 0.01, Mann-Whitney test; #p < 0.01, Levene test. n = 495 (control), 737 (Dicer$^{+/-}$) cells from three different sections. Scale bar, 24 μm. Data are mean + SEM. See also Figure S2.

feedback network indicates that knockdown of either miR-20a/b or miR-23a can increase the expression level and variance of cyclin D1 (Figure 3B). This suggests that the feedback network regulates developmental-stage-specific cyclin D1 expression to control the transition from proliferation to neuronal differentiation.

We tested these feedback relations between cyclin D1 and miR-20a/b and miR-23a. We used in utero electroporation

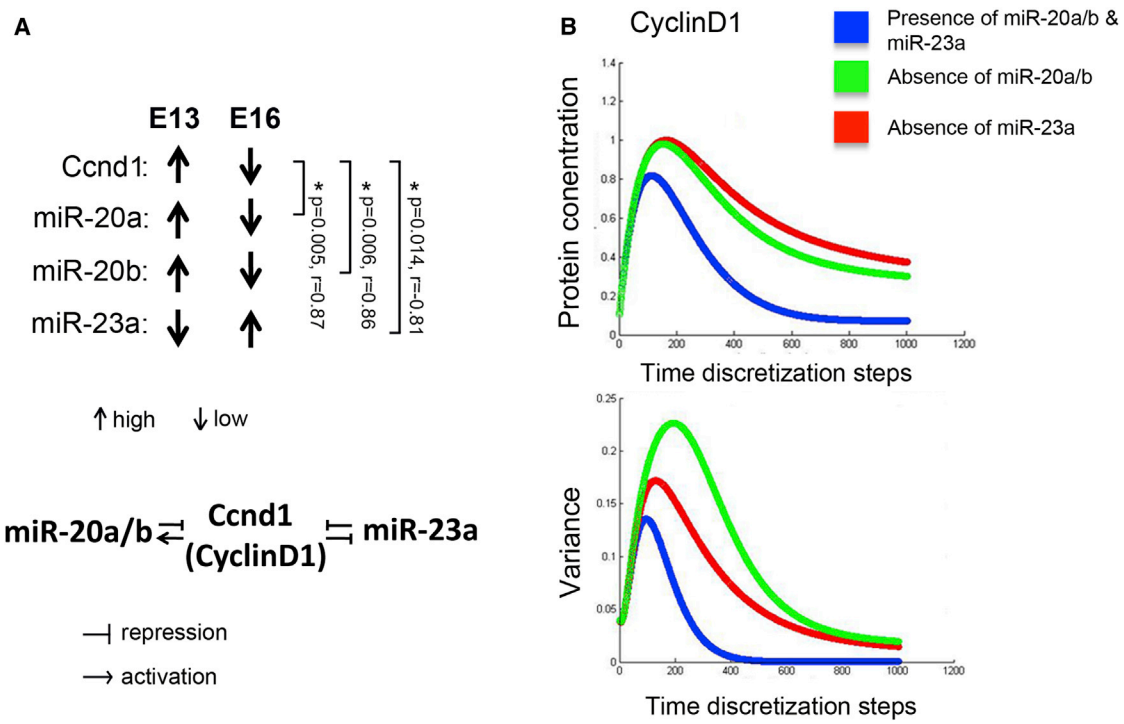

Figure 3. Derivation of Cyclin D1 and miRNA Feedback Network

(A) Top: relative abundance of Ccnd1 and corresponding miRNAs at E13 versus E16, determined by microarray and qPCR (see also Figure S1D). *p < 0.05, Pearson's product moment correlation test for association; p, p value; r, Pearson's correlation coefficient. Normalized expression levels from microarray data were used for correlation tests. n = 8 (four E13, four E16). Bottom: derived Cyclin D1-miRNA interacting network.

(B) Mathematical modeling of the network shown in (A). Top: cyclin D1 concentration in a dynamical system. Bottom: variance of cyclin D1 calculated upon Gaussian initial value perturbation.

(IUE) to knock down cyclin D1 in the cortex at E13, when its endogenous level is higher, and overexpress cyclin D1 at E15, when it is lower. Electroporated cells were isolated by FACS and analyzed by qPCR. Cyclin D1 knockdown yielded reduced miR-20a/b and elevated miR-23a level, while cyclin D1 overexpression exerted the opposite effect (Figure 4A). Interestingly let-7b and some of its family members such as let-7a/c/f also showed differential expression (Figures S1C and S1D). Among these family members, let-7b has been previously identified as a regulator of cyclin D1 in cortical progenitors (Zhao et al., 2010). However, let-7b levels remained unaffected by cyclin D1 overexpression or knockdown (Figure S2D). These data suggest that cyclin D1 can induce miR-20a/b and repress miR-23a expression while having no effect on other regulatory miRNAs such as let-7b.

This regulatory effect of cyclin D1 on its corresponding miRNAs may be an emerging property of the network, including their direct interactions. In addition to its cell-cycle roles, cyclin D1 functions as transcriptional regulator during neurodevelopment (Bienvenu et al., 2010) and has been implicated in homologous recombination-mediated DNA repair (Jirawatnotai et al., 2011). We assessed whether cyclin D1 binds in close proximity to the genomic loci of its corresponding miRNAs. Chromatin immunoprecipitation (ChIP) experiments of cyclin D1 from E13 embryonic cortex revealed in vivo occupancy of cyclin D1 on regulatory regions of miR-20a, miR-20b, and miR-23a (Figure 4B). This suggests that cyclin D1 might transcriptionally regulate these miRNAs. Several sequence-specific transcription factor (TF) binding motifs in cyclin D1-bound genomic regions have been described earlier, and these TFs were shown to interact with cyclin D1 (Bienvenu et al., 2010). We analyzed such conserved TF motifs and identified the Stat3 (signal transducer and activator of transcription 3) binding motif in the cyclin D1-occupied regulatory regions of miR-20a, miR-20b, and miR-23a (Figure S2E). Studies of *Stat3* cortex-specific knockout mice have shown its involvement in the maintenance of cortical neural precursors (Yoshimatsu et al., 2006). Furthermore, Stat3 expression is positively correlated with cyclin D1 in our microarray analysis (Figure S2E).

Conversely, we tested the effect of miRNA inhibition on cyclin D1 protein levels. We first validated miRNA target sites in the 3′ UTR of cyclin D1 (Figure S3A) by luciferase assays in cortical progenitors. Knockdown of miRNA expression using locked nucleic acids (LNA) against miR-20a/b (LNA-20a/b) or miR-23a (LNA-23a) increased luciferase activity, whereas no effects were found in controls harboring mutated 3′ UTR targets. In addition, we performed compensatory mutagenesis analysis where mutations in the miRNA seed region were complementary to the mutated 3′ UTR targets (Figure S3B). We cloned pre-miRNAs and verified their processing into the mature form in cortical

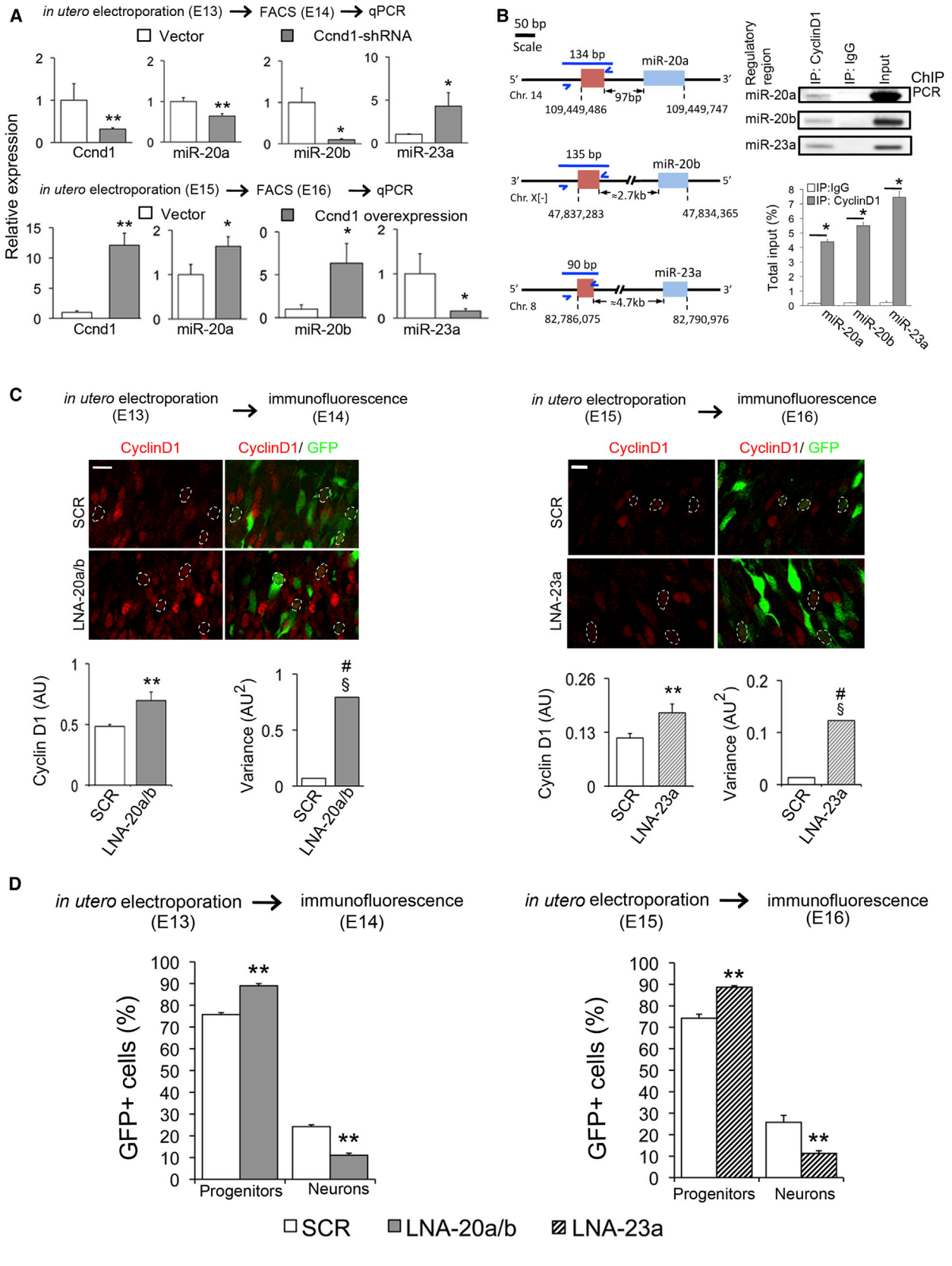

(legend on next page)

progenitors by qPCR (Figure S3C). The complementary miRNA mutations compensated (Figure S3B) the mutations in their targets and reduced luciferase activity to control levels, indicating that the inhibitory effects of these miRNAs on the 3′ UTR of cyclin D1 is direct.

To study these inhibitory effects in vivo, we performed in utero coelectroporation of LNA-20a/b (at E13) or LNA-23a (at E15) along with the GFP reporter and determined the signal intensity of cyclin D1 immunofluorescence 24 hours later. We observed that cyclin D1 immunoreactivity was significantly higher in LNA-20a/b- and in LNA-23a-electroporated progenitors as compared to scrambled LNA (SCR-LNA) (Figure 4C). These experiments demonstrate an inhibitory effect of miR-20a/b and miR-23a on cyclin D1 protein expression. Taken together, these data are consistent with a feedback regulation between cyclin D1 and miR-20a/b or miR-23a (Figure 3A).

We next determined the dynamic expression range of cyclin D1 by measuring its cell-to-cell variation. We observed a significant increase of cyclin D1 expression variance for LNA-23a (9-fold) and LNA-20a/b (11-fold) as compared to SCR (Figure 4C), indicating that these miRNAs constrain the dynamic expression range of cyclin D1.

Finally, we determined the proportion of progenitors and neurons 24 hours following LNA electroporation. We found that in utero electroporation of LNA-20a/b at E13 or LNA-23a at E15 reduced neurogenesis as compared to SCR controls (Figure 4D; Figures S4A–S4C). Correspondingly, the number of progenitors proportionately increased, suggesting an impaired transition from progenitor to neuron. This is also consistent with previously reported increased progenitor proliferation and reduced neurogenesis following cyclin D1 overexpression (Pilaz et al., 2009; Lange et al., 2009). Immunolabeling for Tbr1 further confirmed that LNA-electroporated GFP+ cells in the intermediate zone had committed to a neuronal cell fate and were not misspecified into glia (Figure S4D).

Thus, miR-20a/b and miR-23a regulate the developmental-stage-specific mean and variance of cyclin D1 protein levels in a feedback regulatory network. The logic of this network suggests a fail-safe mechanism for developmental-stage-specific decisions of cortical progenitors to proliferate or to differentiate. Deficiency of these miRNAs increases the dynamic expression range as well as the mean expression level of cyclin D1 and impairs the balance between progenitor proliferation and differentiation. While cyclin D1 and miRNAs 20a/b and 23a can directly regulate each other, each miRNA may have additional targets in the network that are linked to cyclin D1 via direct and indirect interactions. Hence, the feedback regulatory mechanisms to precisely control cyclin D1 expression are properties emerging from the net effects of the direct and indirect network interactions.

In summary, we used a data-driven, hypothesis-free approach and derived integrated feedback loops between specific miRNAs and their target. We identified specific miRNAs that act as a tuner and buffer to confer robustness and adaptability of a crucial gene network during cortical neurogenesis. Failure of these functions may increase the susceptibility to genetically complex neurodevelopmental disorders.

EXPERIMENTAL PROCEDURES

Mice

Tbr2GFP knockin mice have been described previously (Arnold et al., 2009). Dicer conditional heterozygous mice were generated by crossing *Dicer*$^{loxP/loxP}$ with *Nestin*-Cre$^{+/-}$ mice. Mice were maintained in a 12 hr light:dark cycle at temperature 22°C ± 1°C and humidity 60% ± 5%; food and water were supplied ad libitum. Experiments were performed in accordance with French (Ministère de l'Agriculture et de la Forêt, 87-848) and European Economic Community (86-6091) guidelines for the care of laboratory animals and approved by the "Direction Départementale de la Protection des Populations de Paris" (license B75-05-22). The vaginal plug detected in the morning was defined as E0.5.

Cellular Dissociation and FACS

Single-cell suspension from embryonic cortex was prepared by using the Papain Dissociation System (Worthington). FACS was performed with cells resuspended in neurobasal media (without phenol red) (GIBCO) with B27 (Gibco) in a MoFlo XDP system (Beckman Coulter). Summit v5.2 software was used for data analysis. Gating parameters were determined by using side and forward scatter to eliminate dead cells and aggregates and GFP (488 nm) fluorescence to separate GFP+ cells. For cyclin D1 overexpression experiments, red fluorescent protein (RFP) fluorescence (561 nm) was used for sorting. Sorted cells were centrifuged at 1,000 rpm (5 min, 4°C), and RNA was isolated.

RNA Isolation and Microarrays

Total RNA was isolated using the mirVana kit (Ambion). RNA quantity was measured using nanodrop 1000 (Thermo Scientific) and quality determined using bioanalyzer (Agilent). RNA integrity number values were 8–10. A total of 100 ng of total RNA was used for miRNA microarrays (Agilent Mouse Microarray Kit [v2], 8 × 15K) and 150 ng for mRNA microarrays (Illumina BeadChip Array MouseWG-6 v2) experiments.

Figure 4. Experimental Validation of Cyclin D1-miRNA Feedback Network during Neurogenesis

(A) Top: effects of cyclin D1 knockdown and (bottom) overexpression on miRNA expression. n = 3–6 independent experiments (three to four embryonic brains per experiment pooled). *$p < 0.05$, **$p < 0.01$, Student's t test.

(B) Occupancy of cyclin D1 to the nearest regulatory region (left panel) of miR-20a, miR-20b, and miR-23a was verified by ChIP analysis in E13 embryonic cortex using anti-cyclin D1 antibody. PCR primers (blue left and right arrow) and amplicon length are shown. Genomic positions are according to UCSC mm7 mouse genome build. Quantification of enrichment (% total input) in ChIP samples was plotted. n = 3 independent experiments. **$p < 0.01$, Student's t test.

(C) Immunofluorescence intensity analysis of cyclin D1 mean level per cell and variance 24 hours after electroporation of LNA-20a/b at E13 or LNA-23a at E15. SCR, scrambled-LNA. y axis: Cyclin D1 fluorescence intensity normalized to GFP intensity, arbitrary units (AU). #$p < 0.01$, Levene test; §$p < 0.01$, F-test for determining significance for unequal variance. **$p < 0.01$, Welch's t test. n = 114–280 GFP+ cells from three different sections. Representative immuno images are shown (top). Scale bars represent 39 μm (E13) and 30 μm (E16).

(D) Quantification of progenitors and neurons in the embryonic cortex 24 hours after electroporation of LNA-20a/b at E13 (top) and LNA-23a at E15 (bottom). **$p < 0.01$, ANOVA (Bonferroni post-test); n = 3 embryos from different litters. Progenitors: Tbr2+GFP+ cells in the ventricular zone (VZ) and subventricular zone (SVZ) and GFP+Tbr2- cells in the VZ; neurons: GFP+ cells in the intermediate zone and GFP+Tbr2- cells in the SVZ. See also Figure S4.

Data are presented as mean + SEM.

miRNA qPCR Analysis

A TaqMan miRNA assay (Applied Biosystems) specific for each miRNA was used for reverse transcription and further qPCR. The TaqMan reporter was FAMTM dye. Samples were assayed in technical quadruplicate and normalized to snoRNA202 (endogenous control).

For qPCR data analysis, the Pfaffl method (Pfaffl, 2001) was used for relative quantification of gene expression. PCR efficiency of target gene and endogenous control gene has been determined from the slope of the respective standard curve.

Chromatin Immunoprecipitation Analysis

Six E13 embryonic cortices were pooled for each experiment and followed standard ChIP protocol (Weinmann and Farnham, 2002). Previously validated cyclin D1 antibody (HD11) (sc-246, Santa Cruz Biotechnology) (Bienvenu et al., 2005; Cicatiello et al., 2004) was used for ChIP. Sonication (30 s on, 30 s off, 30 min) was performed using Bioruptor (Diagenode), and fragment size ~200–500 bp was verified. A total of 40% (400 μl) of the sonicated DNA was used for anti-cyclin D1 and anti-immunoglobulin G samples, and 2% was used for input samples. A total of 4 μg antibody (cyclin D1 or immunoglobulin G) was used for immunoprecipitation, and blocked Protein G agarose (Millipore) was used for the pull-down step after immunoprecipitation. Precipitated DNA samples were analyzed by PCR (35–38 cycles). Cyclin D1-bound nearest genomic region of miR-20a, miR-20b, and miR-23a was identified from ChIP-chip experimental data (Bienvenu et al., 2010). PCR primers are listed in Supplemental Experimental Procedures.

In Utero Electroporation

IUE was performed as described previously (Lange et al., 2009). Plasmids used for cyclin D1 overexpression (containing RFP reporter) and repression (shRNA-cyclin D1 plasmid, containing GFP reporter) experiments were described previously (Lange et al., 2009). LNA-modified oligonucleotides (miRCURY LNATM miRNA inhibitors) were purchased from Exiqon. Due to the very high level of sequence identity between miR-20a and miR-20b (which differ by 2 nt in a total length of 23 nt), they were targeted by the same LNA inhibitor. A total of 16–20 μM LNA (along with a GFP reporter construct) was used for IUE. The LNA sequences were 5′-GTGTAACACGTC TATACGCCCA-3′ (scramble-miR for control), 5′-CTACCTGCACTATGAG CACTTTG-3′ (for miR-20a/b), and 5′-GGAAATCCCTGGCAATGTGAT-3′ (for miR-23a).

miRNA Target Prediction

A union of miRNA target genes predicted by Targetscan (v 6.0) (Lewis et al., 2005) and PicTar (Krek et al., 2005) was used. These algorithms are based on miRNA target sequence conservation among orthologs, miRNA seed sequence complementarities, free energy calculation, and probabilistic inference on maximum likelihood fit. For the 19 differentially expressed miRNAs, 4,303 mRNA targets were predicted. Among these predicted targets, 2,815 genes were actually expressed in FACS sorted cells. These 2,815 targets were matched with differentially expressed mRNAs (1,501 genes).

WGCNA Summary

Traditionally, expression analysis considers genes in isolation and identifies differentially expressed genes between groups. In contrast, WGCNA (Zhang and Horvath, 2005) considers dependencies of the expression level of one gene on the expression of all others. It exploits the inherent structural organization of the entire transcriptome to reveal its functional organization without any prior hypothesis of data classification. WGCNA is calculating connection strength between genes based on coexpression relations between all pairs of expressed genes across, rather than between, different biological conditions (e.g., developmental stages, genotypes, treatments). This allows the identification of modules of highly connected genes that are associated with specific biological functions. For details, see Supplemental Experimental Procedures.

Pathway Studio

Pathway studio (Nikitin et al., 2003) uses the "ResNet v 9.0" mammalian database (Ariadne Genomics), which contains up-to-date experimentally validated published interactions among genes or proteins to reconstruct molecular networks. Using 371 genes as an input, we explored pathway studio and constructed a network based on the interaction of any two genes by promoter binding and/or mutual expression alterations.

Overrepresentation Analysis

DAVID (the Database for Annotation, Visualization and Integrated Discovery) (Huang et al., 2009) is a bioinformatics resource that comprises gene or protein annotation databases and several analytical tools for extracting biological relations from a list of genes. The DAVID functional annotation tool was used for analyzing KEGG pathway terms overrepresented in WGCNA modules. A Bonferroni adjusted p value < 0.05 was considered significant.

Overrepresentation Analysis for Microcephaly/Macrocephaly Endophenotypes

Gene names associated with "microcephaly" and "macrocephaly" endophenotypes were extracted from the manually curated GenAtlas database (Frézal, 1998) (http://www.genatlas.org), currently containing more than 82,000 reference entries, more than 22,431 gene entries, and 4,350 phenotype entries. A total of 116 and 53 nonredundant gene symbols were found for microcephaly and macrocephaly, respectively. Among these genes, 81 microcephaly genes and 38 macrocephaly genes were found to be expressed in FACS sorted basal progenitors. Microcephaly and macrocephaly enrichment significance in DPMT and CSDM mRNA lists as compared to all genes expressed in basal progenitors was determined by using a hypergeometric distribution. A Bonferroni adjusted p value < 0.05 was considered significant.

Statistical Analysis

Statistical analyses were performed by using R (version 2.14.0) (http://www.R-project.org). Shapiro-Wilk test (Royston, 1982) was performed to test normality. Levene test (based on mean) (without assuming any distribution) and F test (for normal distribution) were performed to test heteroscedasticity. Welch's t test was performed whenever heteroscedasticity existed. Variance, or Var (X), is described by the following equation (Draghichi, 2011):

$$Var(X) = \left(\sum_{i=1}^{n} (X_i - \overline{X})^2\right) \Big/ (n-1)$$

where X_i is an individual measurement, $\overline{X}$ is the mean of all X_i measurements, and n is the total number of measurements.

The variance is defined as the average square difference from the mean. The variance is calculated by taking the differences between each individual value of a set from the mean, squaring the differences, and then dividing the sum of squares by the total number of values in the set.

Mathematical Modeling

Based on the simple model (Figure 3A), a system of coupled nonlinear ordinary differential equations was used for simulations. Parameters and Hill coefficients were adjusted to the experimental data or reasonable estimates from the literature. A detailed method and code is provided in the Supplemental Experimental Procedures.

ACCESSION NUMBERS

The Gene Expression Omnibus (GEO) database accession number for the miRNA and mRNA microarray data sets reported in this paper is GSE45451.

SUPPLEMENTAL INFORMATION

Supplemental information contains Supplemental Experimental Procedures, four figures, and one table and can be found with this article online at http://dx.doi.org/10.1016/j.celrep.2014.05.029.

AUTHOR CONTRIBUTIONS

T.G. and M.G. conceived and designed the experiments and analyzed the data. T.G., J.A., J.N., H.E., C.M., T.L., I.M., L.S., M.D., T.I., S.J.A., P.G., and

F.C. performed experiments. T.G. performed bioinformatics analyses. T.G., C.S., and A.G.B. performed the mathematical modeling. A.H.C. performed data mining of the GenAtlas database. T.G., F.C., S.J.A., A.H.C., and M.G. wrote the manuscript.

ACKNOWLEDGMENTS

This work was supported by grants from Agence Nationale de la Recherche-ANR, Projet ANR- 09-MNPS-029 'TransCTX': PO08978 (to M.G.), Ecole des Neurosciences de Paris-ENP (to M.G.), INSERM/CNRS ATIP-AVENIR programme (to M.G.), *Fondation pour la Recherche Médicale en France*-FRM: SPF20090515606 (to T.G.), DFG Collaborative Research Center SFB655 (subproject A20), Center for Regenerative Therapies and Medical Faculty of the TU Dresden (to F.C., J.A., and M.D.), ANR and the Institut des Hautes Etudes Scientifiques (to A.G.B.), DFG (AR 732/1-1) (to S.J.A.), and APHP (Contrat Hospitalier de Recherche Translationnelle) and ARC (SF120121205530) (to P.G.). We thank Annie Munier (UPMC) for technical support of FACS experiments, Mythili Savariradjane (IFM) for fluorescence microscopy, Drs. Dilair Baban and Ana Teixeira (Welcome Trust Centre, Oxford University) for microarray experiments, Dr. Beena Pillai (IGIB) for providing expression vectors, Dr. Robert Hevner (University of Washington, Seattle) for providing Tbr1 antibody, and Drs. Anthony Mathelier and Wyeth W. Wasserman (University of British Columbia, Vancouver) for fruitful discussion and advice during probabilistic analysis of TF motifs.

Received: November 7, 2013
Revised: February 18, 2014
Accepted: May 14, 2014
Published: June 12, 2014

REFERENCES

Arnold, S.J., Sugnaseelan, J., Groszer, M., Srinivas, S., and Robertson, E.J. (2009). Generation and analysis of a mouse line harboring GFP in the Eomes/Tbr2 locus. Genesis *47*, 775–781.

Baek, D., Villén, J., Shin, C., Camargo, F.D., Gygi, S.P., and Bartel, D.P. (2008). The impact of microRNAs on protein output. Nature *455*, 64–71.

Bian, S., Hong, J., Li, Q., Schebelle, L., Pollock, A., Knauss, J.L., Garg, V., and Sun, T. (2013). MicroRNA cluster miR-17-92 regulates neural stem cell expansion and transition to intermediate progenitors in the developing mouse neocortex. Cell Reports *3*, 1398–1406.

Bienvenu, F., Barré, B., Giraud, S., Avril, S., and Coqueret, O. (2005). Transcriptional regulation by a DNA-associated form of cyclin D1. Mol Biol Cell *16*, 1850–1858.

Bienvenu, F., Jirawatnotai, S., Elias, J.E., Meyer, C.A., Mizeracka, K., Marson, A., Frampton, G.M., Cole, M.F., Odom, D.T., Odajima, J., et al. (2010). Transcriptional role of cyclin D1 in development revealed by a genetic-proteomic screen. Nature *463*, 374–378.

Caviness, V.S., Jr. (1982). Neocortical histogenesis in normal and reeler mice: a developmental study based upon [3H]thymidine autoradiography. Brain Res. *256*, 293–302.

Cicatiello, L., Addeo, R., Sasso, A., Altucci, L., Petrizzi, V.B., Borgo, R., Cancemi, M., Caporali, S., Caristi, S., Scafoglio, C., et al. (2004). Estrogens and progesterone promote persistent CCND1 gene activation during G1 by inducing transcriptional derepression via c-Jun/c-Fos/estrogen receptor (progesterone receptor) complex assembly to a distal regulatory element and recruitment of cyclin D1 to its own gene promoter. Mol. Cell. Biol. *24*, 7260–7274.

de Pontual, L., Yao, E., Callier, P., Faivre, L., Drouin, V., Cariou, S., Van Haeringen, A., Geneviève, D., Goldenberg, A., Oufadem, M., et al. (2011). Germline deletion of the miR-17∼92 cluster causes skeletal and growth defects in humans. Nat. Genet. *43*, 1026–1030.

Dehay, C., and Kennedy, H. (2007). Cell-cycle control and cortical development. Nat. Rev. Neurosci. *8*, 438–450.

Draghichi, S. (2011). Statistics and Data Analysis for Microarrays Using R and Bioconductor (Boca Raton: Chapman & Hall/CRC Press), p. 217.

Englund, C., Fink, A., Lau, C., Pham, D., Daza, R.A., Bulfone, A., Kowalczyk, T., and Hevner, R.F. (2005). Pax6, Tbr2, and Tbr1 are expressed sequentially by radial glia, intermediate progenitor cells, and postmitotic neurons in developing neocortex. J. Neurosci. *25*, 247–251.

Enver, T., Pera, M., Peterson, C., and Andrews, P.W. (2009). Stem cell states, fates, and the rules of attraction. Cell Stem Cell *4*, 387–397.

Frézal, J. (1998). Genatlas database, genes and development defects. C. R. Acad. Sci. III *321*, 805–817.

Hornstein, E., and Shomron, N. (2006). Canalization of development by microRNAs. Nat. Genet. Suppl. *38*, S20–S24.

Huang, W., Sherman, B.T., and Lempicki, R.A. (2009). Systematic and integrative analysis of large gene lists using DAVID bioinformatics resources. Nat. Protoc. *4*, 44–57.

Jirawatnotai, S., Hu, Y., Michowski, W., Elias, J.E., Becks, L., Bienvenu, F., Zagozdzon, A., Goswami, T., Wang, Y.E., Clark, A.B., et al. (2011). A function for cyclin D1 in DNA repair uncovered by protein interactome analyses in human cancers. Nature *474*, 230–234.

Krek, A., Grün, D., Poy, M.N., Wolf, R., Rosenberg, L., Epstein, E.J., MacMenamin, P., da Piedade, I., Gunsalus, K.C., Stoffel, M., and Rajewsky, N. (2005). Combinatorial microRNA target predictions. Nat. Genet. *37*, 495–500.

Lange, C., Huttner, W.B., and Calegari, F. (2009). Cdk4/cyclinD1 overexpression in neural stem cells shortens G1, delays neurogenesis, and promotes the generation and expansion of basal progenitors. Cell Stem Cell *5*, 320–331.

Lewis, B.P., Burge, C.B., and Bartel, D.P. (2005). Conserved seed pairing, often flanked by adenosines, indicates that thousands of human genes are microRNA targets. Cell *120*, 15–20.

Li, X., Cassidy, J.J., Reinke, C.A., Fischboeck, S., and Carthew, R.W. (2009). A microRNA imparts robustness against environmental fluctuation during development. Cell *137*, 273–282.

Nikitin, A., Egorov, S., Daraselia, N., and Mazo, I. (2003). Pathway studio—the analysis and navigation of molecular networks. Bioinformatics *19*, 2155–2157.

Nowakowski, T.J., Fotaki, V., Pollock, A., Sun, T., Pratt, T., and Price, D.J. (2013). MicroRNA-92b regulates the development of intermediate cortical progenitors in embryonic mouse brain. Proc. Natl. Acad. Sci. USA *110*, 7056–7061.

Oldham, M.C., Konopka, G., Iwamoto, K., Langfelder, P., Kato, T., Horvath, S., and Geschwind, D.H. (2008). Functional organization of the transcriptome in human brain. Nat. Neurosci. *11*, 1271–1282.

Pfaffl, M.W. (2001). A new mathematical model for relative quantification in real-time RT-PCR. Nucleic Acids Res. *29*, e45.

Pilaz, L.-J., Patti, D., Marcy, G., Ollier, E., Pfister, S., Douglas, R.J., Betizeau, M., Gautier, E., Cortay, V., Doerflinger, N., et al. (2009). Forced G1-phase reduction alters mode of division, neuron number, and laminar phenotype in the cerebral cortex. Proc. Natl. Acad. Sci. USA *106*, 21924–21929.

Royston, J.P. (1982). Algorithm AS 181: the *W* test for normality. Appl. Stat. *181*, 176–180.

Salomoni, P., and Calegari, F. (2010). Cell cycle control of mammalian neural stem cells: putting a speed limit on G1. Trends Cell Biol. *20*, 233–243.

Selbach, M., Schwanhäusser, B., Thierfelder, N., Fang, Z., Khanin, R., and Rajewsky, N. (2008). Widespread changes in protein synthesis induced by microRNAs. Nature *455*, 58–63.

Sieber, P., Wellmer, F., Gheyselinck, J., Riechmann, J.L., and Meyerowitz, E.M. (2007). Redundancy and specialization among plant microRNAs: role of the MIR164 family in developmental robustness. Development *134*, 1051–1060.

Staton, A.A., Knaut, H., and Giraldez, A.J. (2011). miRNA regulation of Sdf1 chemokine signaling provides genetic robustness to germ cell migration. Nat. Genet. *43*, 204–211.

Tsang, J., Zhu, J., and van Oudenaarden, A. (2007). MicroRNA-mediated feedback and feedforward loops are recurrent network motifs in mammals. Mol. Cell *26*, 753–767.

Volvert, M.-L., Rogister, F., Moonen, G., Malgrange, B., and Nguyen, L. (2012). MicroRNAs tune cerebral cortical neurogenesis. Cell Death Differ. *19*, 1573–1581.

Weinmann, A.S., and Farnham, P.J. (2002). Identification of unknown target genes of human transcription factors using chromatin immunoprecipitation. Methods *26*, 37–47.

Wu, C.-I., Shen, Y., and Tang, T. (2009). Evolution under canalization and the dual roles of microRNAs: a hypothesis. Genome Res. *19*, 734–743.

Wu, S., Huang, S., Ding, J., Zhao, Y., Liang, L., Liu, T., Zhan, R., and He, X. (2010). Multiple microRNAs modulate p21Cip1/Waf1 expression by directly targeting its 3′ untranslated region. Oncogene *29*, 2302–2308.

Yoshimatsu, T., Kawaguchi, D., Oishi, K., Takeda, K., Akira, S., Masuyama, N., and Gotoh, Y. (2006). Non-cell-autonomous action of STAT3 in maintenance of neural precursor cells in the mouse neocortex. Development *133*, 2553–2563.

Zhang, B., and Horvath, S. (2005). A general framework for weighted gene co-expression network analysis. Stat. Appl. Genet. Mol. Biol. *4*, Article17.

Zhao, C., Sun, G., Li, S., Lang, M.-F., Yang, S., Li, W., and Shi, Y. (2010). MicroRNA let-7b regulates neural stem cell proliferation and differentiation by targeting nuclear receptor TLX signaling. Proc. Natl. Acad. Sci. USA *107*, 1876–1881.